Broadband absorption of semiconductor nanowire arrays for photovoltaic applications

2012 J. Opt. 14 024004

(http://iopscience.iop.org/2040-8986/14/2/024004)

IOP Publishing Journal of Optics
J. Opt. **14** (2012) 024004 (7pp) doi:10.1088/2040-8978/14/2/024004

Broadband absorption of semiconductor nanowire arrays for photovoltaic applications

Ningfeng Huang, Chenxi Lin and Michelle L Povinelli

Ming Hsieh Department of Electrical Engineering, University of Southern California, 3561 Watt Way, VHE 309, Los Angeles, CA 90089-0106, USA

E-mail: ningfenh@usc.edu

Received 8 July 2011, accepted for publication 7 September 2011
Published 12 January 2012
Online at stacks.iop.org/JOpt/14/024004

Abstract
We use electromagnetic simulations to carry out a systematic study of broadband absorption in vertically-aligned semiconductor nanowire arrays for photovoltaic applications. We study six semiconductor materials that are commonly used for solar cells. We optimize the structural parameters of each nanowire array to maximize the ultimate efficiency. We plot the maximal ultimate efficiency as a function of height to determine how it approaches the perfect-absorption limit. We further show that the ultimate efficiencies of optimized nanowire arrays exceed those of equal-height thin films for all six materials and over a wide range of heights from 100 nm to 100 μm.

Keywords: nanowire array, absorption enhancement, photovoltaics

(Some figures in this article are in colour only in the electronic version)

1. Introduction

Semiconductor nanowire solar cells are promising candidates for next-generation, thin-film photovoltaic devices due to their attractive anti-reflection and light-trapping properties. Recent experimental work has demonstrated vertically-aligned semiconductor nanowire arrays in silicon [1–9], germanium [10], various direct band gap materials [11–18], and combined systems [19–21]. Nanowire arrays can be fabricated by either top-down [1, 2, 22] or bottom-up methodologies [3, 10, 12, 21]. By using different patterning techniques [10, 14, 15, 17, 23] regular arrays of nanowires have been achieved. Junctions have been made between semiconductor nanowires and substrate [12] and between the core and shell of semiconductor nanowires [13, 23]. Experiments on hybrid nanowire/polymer systems have also been conducted [24, 25].

In this work, we use electromagnetic simulations to map out the limiting efficiencies of nanowire solar cells. We focus on structures for which the nanowires themselves function as the broadband absorber. Ideally, a photovoltaic cell will absorb as large a fraction of incident photons as possible over the entire solar spectrum. Previous work has shown that the structural parameters of the nanowire array strongly influence the broadband absorption [26, 27]. Given proper design, light-trapping effects yield high broadband absorption, even for nanowire heights shorter than the bulk absorption length. Specifically, we have shown that the ultimate efficiency of an optimized silicon nanowire array exceeds that of an equal-height thin film, even though it contains less absorptive material [27]. Similar optimization work has been carried out for silicon nanowires on silicon thin films [28], as well as for InP/InAs [29], InP [30] and GaAs/AlGaAs [31] nanowire arrays.

However, previous work has been restricted either to a fixed height or to a very limited height range. The dependence of broadband absorption on height has not been determined. It is important to determine the extent to which light trapping can be used to minimize material usage while maintaining acceptably high photovoltaic efficiency. Material usage can have important implications for the cost of a process. For bottom-up growth methods such as MOCVD, for example, it is of particular interest to know what heights are sufficient to guarantee acceptable efficiencies, given the potentially time-

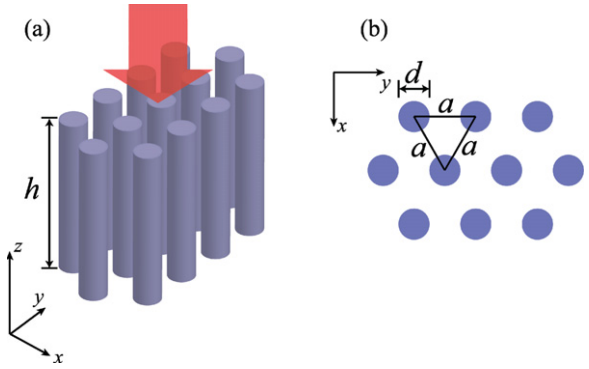

Figure 1. Schematic of a vertically-aligned semiconductor nanowire array. (a) Perspective view. (b) Cross-sectional view.

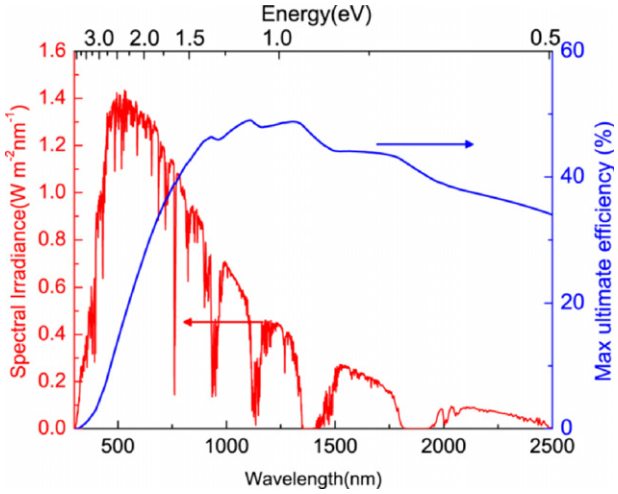

Figure 2. Direct + circumsolar spectral irradiance AM1.5 (red line), reprinted from [41], and the perfect-absorption limit of the ultimate efficiency (blue line).

consuming and expensive nature of the growth process. For photovoltaic space applications, the material volume affects the total weight, which correlates with the launch cost. From a scientific standpoint, it is of interest to determine how fast the efficiency degrades as the height of a nanowire array is reduced, in order to determine whether optimized structures will allow approach to an 'ultra-thin' film limit.

In this paper, we systematically study the broadband absorption of vertically-aligned nanowire arrays made of six common photovoltaic materials. For each material, we study how the ultimate efficiency depends on the height of the array. At each value of height, we optimize the structural parameters of the array to maximize the broadband absorption. Thus, the results we present concisely describe the trade-offs between material usage and maximum achievable efficiency in semiconductor nanowire array solar cells. We further compare the optimized nanowire arrays to thin films of the same height and show that for all six materials, and over the entire range of heights tested (100 nm–100 μm), the ultimate efficiencies of the arrays exceed those of equal-height thin films. Our results suggest that nanowire array solar cells hold strong potential for the development of next-generation, thin-film solar cells.

2. Methods

Figure 1 shows a schematic of a vertically-aligned semiconductor nanowire array. The array is illuminated by sunlight from the top, as indicated by the red arrow in figure 1(a). The electric field of the incident light is polarized in either the x or the y direction. As shown in figure 1(b), nanowires with diameter d are arranged in a hexagonal lattice with lattice constant a.

We consider nanowire arrays composed of one of six common photovoltaic materials. Among the materials considered, silicon and germanium are indirect band gap materials, while GaAs, InP, $In_{0.48}Ga_{0.52}P$, and CdTe are direct band gap materials. The optical constants (refractive indices and absorption lengths) are taken from the literature: Si [32], Ge [32], GaAs [32], InP [33], $In_{0.48}Ga_{0.52}P$ [34], and CdTe [35]. Si has a relatively large absorption length in the 400–1100 nm wavelength range compared to the other materials.

We use the ISU-TMM simulation package [36, 37], an implementation of the transfer matrix method [38, 39], to calculate the broadband absorption of semiconductor nanowire arrays. The software can determine the wavelength-dependent transmittance $T(\lambda)$ and reflectance $R(\lambda)$. The absorptance spectrum $A(\lambda)$ is obtained from the relation $A(\lambda) = 1 - T(\lambda) - R(\lambda)$. We average the results for x- and y-polarized incident light. The spectral resolution is chosen to be 5 nm in the wavelength range of interest.

We use the ultimate efficiency [40] to quantify the broadband absorption, as in previous work [26, 27]. The ultimate efficiency is given by

$$\eta = \frac{\int_{300\text{ nm}}^{\lambda_g} I(\lambda)A(\lambda)\frac{\lambda}{\lambda_g}\,d\lambda}{\int_{300\text{ nm}}^{4000\text{ nm}} I(\lambda)\,d\lambda}, \tag{1}$$

where λ is the wavelength, and λ_g is the wavelength corresponding to the band gap of the semiconductor. $I(\lambda)$ is the ASTM AM1.5 solar spectral irradiance [41], which is plotted as a red line in figure 2. $A(\lambda)$ is the absorption spectrum. We set the lower limit of integration to 300 nm in equation (1) because the solar irradiance is negligible below this value. The ultimate efficiency is an upper bound on the achievable efficiency of a solar cell, assuming that each absorbed photon with energy greater than the band gap produces exactly one electron–hole pair at the energy of the gap, $E_g = hc/\lambda_g$. The ultimate efficiency can be related to the maximum short circuit current by assuming perfect carrier collection efficiency, i.e., every photogenerated carrier can reach the electrodes and contribute to the photocurrent. Within this approximation, we do not explicitly consider the junction geometry. In this case,

$$J_{sc} = \int_{300\text{ nm}}^{\lambda_g} I(\lambda)A(\lambda)\frac{e\lambda}{hc}\,d\lambda = \eta\frac{e\lambda_g}{hc}\int_{300\text{ nm}}^{4000\text{ nm}} I(\lambda)\,d\lambda. \tag{2}$$

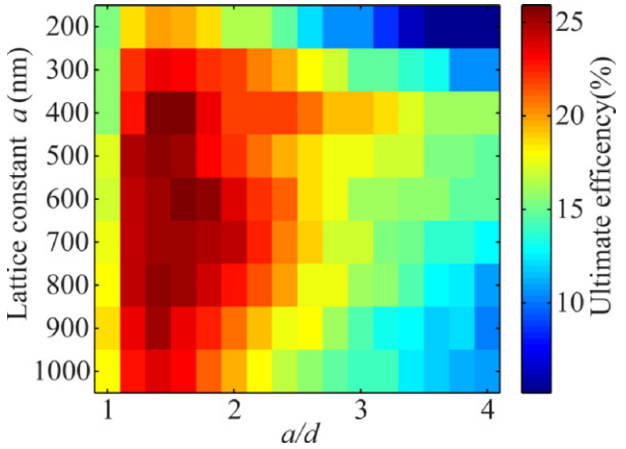

Figure 3. Optimization of the ultimate efficiency with respect to the structural parameters for a silicon nanowire array of 3 μm height.

In the case of perfect absorption, we may set $A(\lambda) = 1$ in equation (1) to obtain the limiting value of ultimate efficiency [40], $\eta_{\max}$. The value of $\eta_{\max}$ is plotted as a function of E_g in figure 2 and obtains a maximum of 49% for a band gap of 1.12 eV.

For nanowire arrays, as for any realistic structure, the ultimate efficiency will always be less than $\eta_{\max}$ due to incomplete absorption. Below, we determine the extent to which structural optimization of a nanowire array can yield efficiency values approaching the perfect-absorption limit. Moreover, we determine the optimized ultimate efficiency as a function of nanowire height.

We optimize the ultimate efficiencies of nanowire arrays with respect to the structural parameters as follows. For fixed nanowire height h, we vary the lattice constant a and the ratio of the lattice constant to diameter, a/d. Seven height values were used: 100 nm, 300 nm, 1 μm, 3 μm, 10 μm, 30 μm and 100 μm. Figure 3 shows an example of a parameter sweep for 3 μm long silicon nanowire arrays. The lattice constant was varied from 200 to 1000 nm in steps of 100 nm and the a/d parameter was varied from 1 (for which the nanowires touch) to 4 in steps of 0.2. The value of the ultimate efficiency is given by the color bar and depends strongly on the structural parameters. In this specific case, the ultimate efficiency varies from a minimum of 5% to a maximum of 26% in the parameter space we consider. Below, we refer to the maximum value of ultimate efficiency, optimized over a and a/d for a particular material and nanowire height, as the optimized ultimate efficiency.

3. Results and discussion

In figure 4(a), we plot the optimized ultimate efficiency as a function of height for all six materials considered. For each material, the optimized ultimate efficiency increases with increasing height of the nanowire array. For the direct band gap materials (GaAs, InP, InGaP, CdTe), the ultimate efficiency increases quickly and is relatively flat for heights above 5 μm. For Si, which is an indirect band gap material, the ultimate efficiency slowly increases over the entire range shown (up to 100 μm). The data for Ge represent an intermediate case.

In figure 4(b), we plot the optimized ultimate efficiency as a function of bandgap energy. The black solid line is the perfect-absorption limit of ultimate efficiency ($\eta_{\max}$), identical to the blue line in figure 2. The colored symbols represent identical data to figure 4(a). The data for each set of nanowire arrays are aligned to the bandgap energy of the constituent material. Different colors represent different heights of the nanowire array. From this plot, the saturation behavior of the ultimate efficiency may be clearly observed. For direct band gap materials, the optimized ultimate efficiency approaches the perfect-absorption limit much more quickly than for indirect band gap materials. For the materials studied, an optimized nanowire array of 3 μm height provides an ultimate efficiency that is >92% of the perfect-absorption limit for InP, GaAs, CdTe, and GaInP, while only 53% for Si and 78% for Ge.

Each data point in figures 4(a) and (b) is obtained by optimizing the structural parameters of the nanowire array to maximize the ultimate efficiency. The optimal values of a and a/d are shown in figures 5(a) and (b), respectively. Different

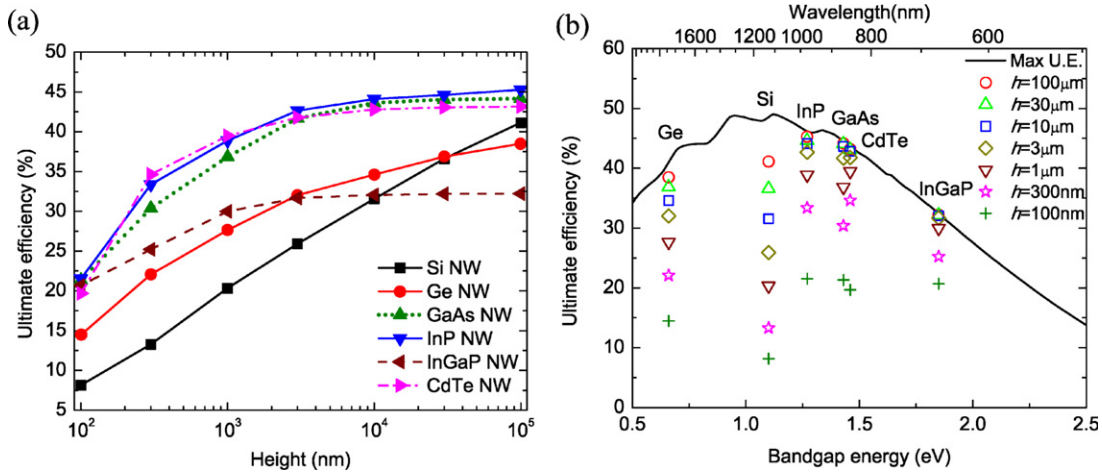

Figure 4. Optimized ultimate efficiencies for nanowire arrays composed of different materials: (a) shown as a function of array height; (b) shown as a function of the bandgap energy of the material.

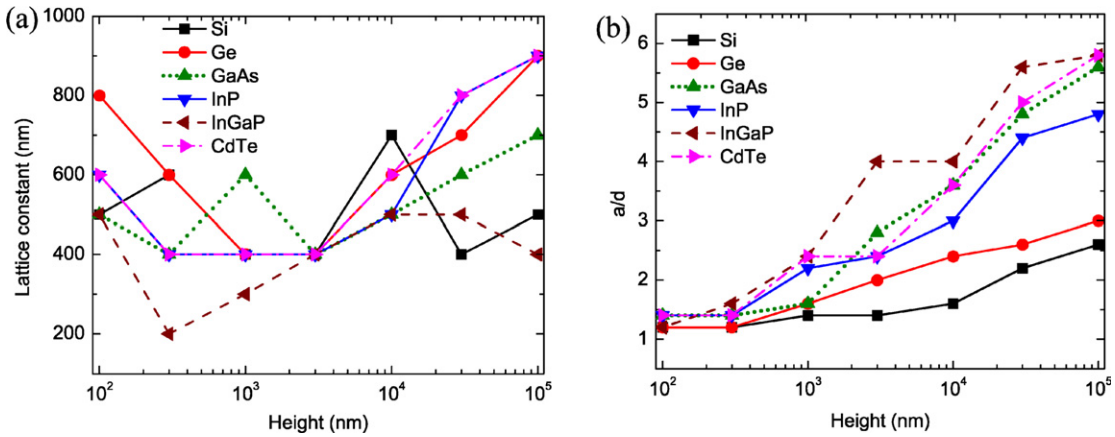

Figure 5. Optimal structural parameters for different heights of different materials: (a) lattice constant; (b) a/d ratio.

color lines represent different materials. From figure 5(a), we observe that there is no obvious trend in the optimal lattice constant. However, most values are comparable to the wavelength of visible light (∼400–700 nm). Figure 5(b) shows that the optimal value of a/d increases with increasing nanowire height. Larger values of a/d correspond to sparser arrays. Intuitively, as the nanowire height increases, it becomes comparable to or larger than the absorption length in the material. In this limit that the nanowire height exceeds the absorption length over the whole solar spectrum, the ultimate efficiency will be maximized by minimizing the reflection from the top surface, which may be achieved by increasing a/d. From figure 5(b), it may also be observed that the optimal value of a/d increases more quickly with length for direct band gap materials than for Si and Ge.

In figure 6, we compare the performance of optimal nanowire arrays to thin films of the same height. The plot shows that in the entire height range we consider, optimal nanowire arrays have higher ultimate efficiencies than their thin-film counterparts. This holds true even though the nanowires contain a smaller volume of absorbing materials than the thin films. Nanowire structures tend to have a lower reflection from their top surface than a thin film. Moreover, the nanowires can also couple normally incident light into modes that propagate in the plane of the array [27], a form of light trapping.

Above, we have considered free-standing nanowire arrays in air. The methods we use can be straightforwardly adapted to model particular choices of substrate material, contact geometries and materials. As one example of a more complex geometry, we consider the effect of a substrate on the ultimate efficiency. We choose GaAs as a representative direct band gap material and compare three possible substrate choices (no substrate, GaAs substrate, and glass substrate) using FDTD calculations. We assume that the solar cell is designed such that photogenerated carriers are collected only from the nanowire region. Hence, we calculate the ultimate efficiency using $A(\lambda)$ for the nanowire region alone. Absorption spectra, $A(\lambda)$, are obtained from the FDTD simulation by monitoring the flux difference between flux planes located above and below the nanowire array. We vary the height of the nanowire array as in the calculations above. For each height, we use the optimal structural parameters from figure 5, which were obtained for the free-floating structure.

The black line in figure 7 shows the ultimate efficiency of GaAs nanowire arrays without a substrate, corresponding to the green dotted line in figure 4(a). The red and blue lines represent the ultimate efficiencies achieved for a GaAs and a glass substrate ($n = 1.55$) underneath the nanowires, respectively. As one would expect, the glass substrate has a smaller effect on the ultimate efficiency than the higher-index, GaAs substrate. Moreover, we observe that when the height of the nanowire array is longer than about 3 μm, the effect of a glass or GaAs substrate on the ultimate efficiency is minimal. Intuitively, when the height of the nanowire array is large enough, most light will be absorbed without reflecting from the interface between the nanowires and the substrate. We observe that this height scale is similar to that at which the ultimate efficiency of the nanowire array approaches the perfect-absorption limit (figure 4(b)). We note that the ultimate efficiencies shown by the blue and red lines in figure 7 are not necessarily the maximum values achievable in the presence of a substrate; re-optimizing the structural parameters for a particular substrate of interest is likely to increase the ultimate efficiency.

4. Conclusions

In summary, we use electromagnetic simulation tools to quantitatively determine how the ultimate efficiency of optimized semiconductor nanowire arrays approaches the perfect-absorption limit as a function of nanowire height. Moreover, we demonstrate that optimized nanowire arrays in six different materials and for a range of heights from 100 nm to 100 μm all outperform unpatterned thin films of equal height. The results will assist in the design of highly-efficient nanowire solar cells, while minimizing material usage.

In the work above, we have considered nanowire arrays consisting of a single semiconductor material. Of the materials

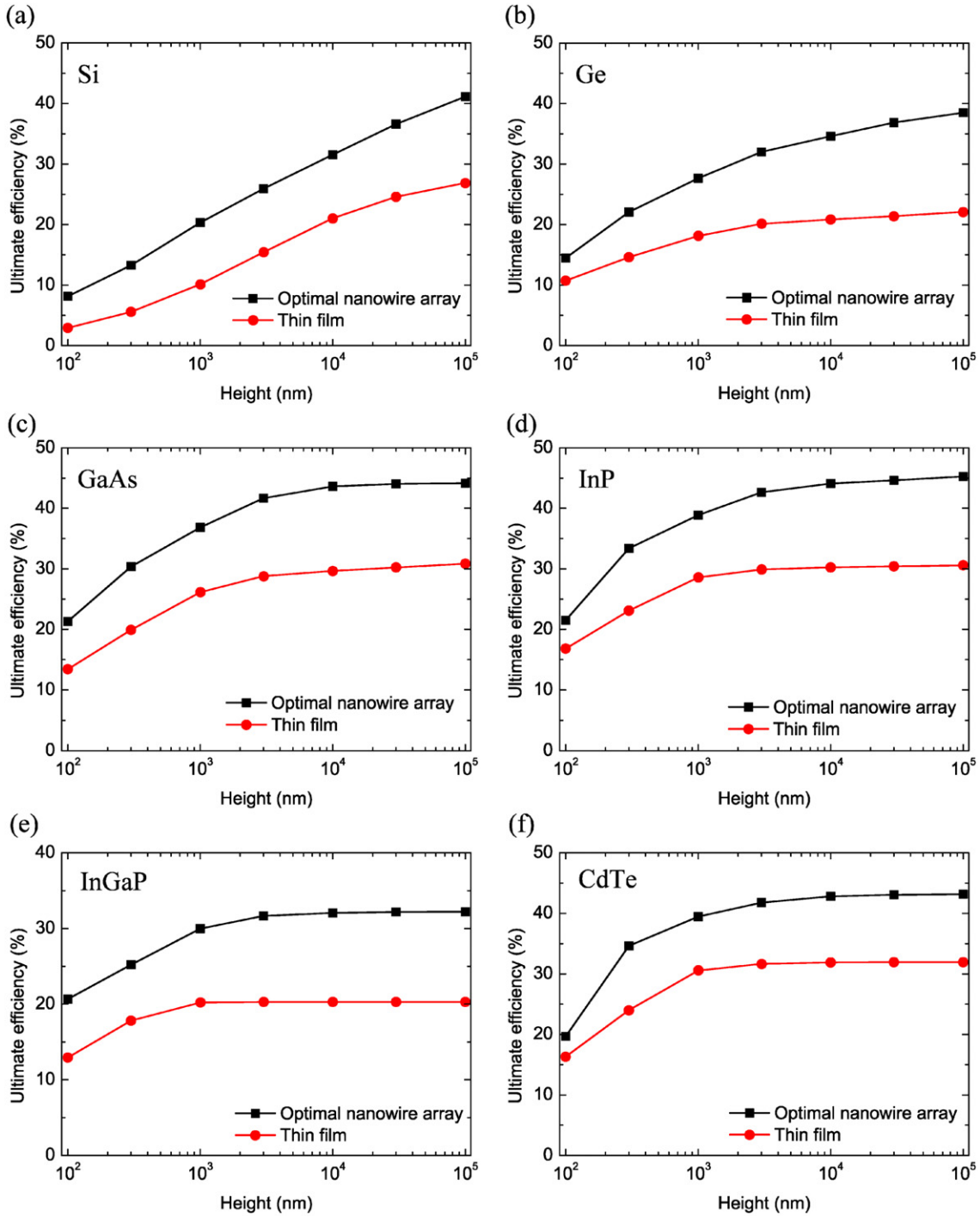

Figure 6. Comparison of the ultimate efficiencies of optimized (a) Si, (b) Ge, (c) GaAs, (d) InP, (e) InGaP, and (f) CdTe nanowire arrays with the ultimate efficiencies of thin films made of the same material and of the same height.

considered, GaAs, $In_{0.48}Ga_{0.52}P$ and Ge are commonly used in triple-junction solar cells. In future work, we aim to extend our modeling to multijunction nanowire geometries. Moreover, III–V nanowire systems allow the growth of non-lattice-matched structures, increasing the range of materials that can be used for multijunction cells. The development of design rules for such structures is an important area of further research.

The incorporation of both optical and electrical properties in increasingly detailed models will play an important role in interpreting experimental results and guiding cell design. In this study, we calculate the ultimate efficiency, which depends only on broadband absorption (equation (1)). The collection efficiency of photogenerated carriers is not explicitly considered. The electrical transport properties of the nanowire will depend on the junction design. Moreover, for small wire

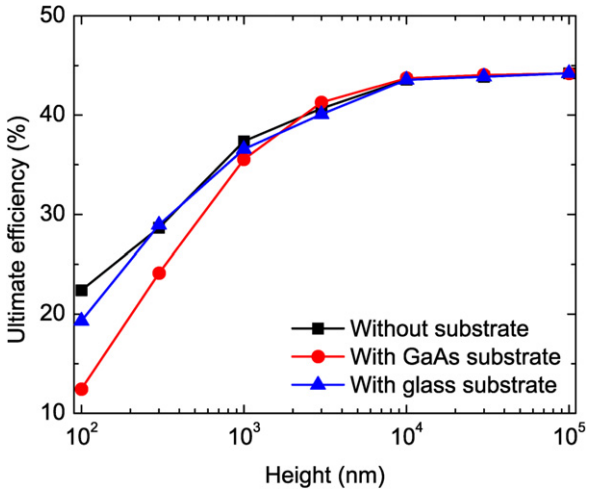

Figure 7. Effect of the substrate on the absorption in nanowire arrays.

sizes, nanoscale size effects on the carrier distribution [42, 43] may affect the optical absorption and electrical transport, modifying the efficiency. These topics are areas for future research.

Acknowledgments

The authors acknowledge helpful discussions with Dan Dapkus. Ningfeng Huang was funded by a USC Annenberg Fellowship. Chenxi Lin and Michelle Povinelli were funded in part by the Center for Energy Nanoscience, an Energy Frontiers Research Center funded by the US Department of Energy, Office of Science, Office of Basic Energy Sciences, under Award DE-SC0001013. Computing resources were provided by the University of Southern California Center for High Performance Computing and Communication (www.usc.edu/hpcc).

References

[1] Dai Y-A *et al* 2010 Subwavelength Si nanowire arrays for self-cleaning antireflection coatings *J. Mater. Chem.* **20** 10924–30
[2] Garnett E C and Yang P 2008 Silicon nanowire radial p–n junction solar cells *J. Am. Chem. Soc.* **130** 9224–5
[3] Gunawan O and Guha S 2009 Characteristics of vapor–liquid–solid grown silicon nanowire solar cells *Sol. Energy Mater. Sol. Cells* **93** 1388–93
[4] Peng K *et al* 2005 Aligned single-crystalline Si nanowire arrays for photovoltaic applications *Small* **1** 1062–7
[5] Tsakalakos L *et al* 2007 Silicon nanowire solar cells *Appl. Phys. Lett.* **91** 233117
[6] Lu Y and Lal A 2010 High-efficiency ordered silicon nano-conical-frustum array solar cells by self-powered parallel electron lithography *Nano Lett.* **10** 4651–6
[7] Kelzenberg M D *et al* 2011 High-performance Si microwire photovoltaics *Energy Environ. Sci.* **4** 866–71
[8] Muskens O L *et al* 2008 Design of light scattering in nanowire materials for photovoltaic applications *Nano Lett.* **8** 2638–42
[9] Stelzner T *et al* 2008 Silicon nanowire-based solar cells *Nanotechnology* **19** 295203
[10] Fan Z *et al* 2010 Ordered arrays of dual-diameter nanopillars for maximized optical absorption *Nano Lett.* **10** 3823–7
[11] Caram J *et al* 2010 Electrical characteristics of core–shell p–n GaAs nanowire structures with Te as the n-dopant *Nanotechnology* **21** 134007
[12] Cirlin G *et al* 2010 Photovoltaic properties of p-doped GaAs nanowire arrays grown on n-type GaAs(111)B substrate *Nanoscale Res. Lett.* **5** 360–3
[13] Colombo C *et al* 2009 Gallium arsenide p–i–n radial structures for photovoltaic applications *Appl. Phys. Lett.* **94** 173108
[14] Diedenhofen S L *et al* 2011 Strong geometrical dependence of the absorption of light in arrays of semiconductor nanowires *ACS Nano* **5** 2316–23
[15] Aurélie P *et al* 2010 Generic nano-imprint process for fabrication of nanowire arrays *Nanotechnology* **21** 065305
[16] Fan Z *et al* 2009 Three-dimensional nanopillar-array photovoltaics on low-cost and flexible substrates *Nature Mater.* **8** 648–53
[17] Goto H *et al* 2009 Growth of core–shell InP nanowires for photovoltaic application by selective-area metal organic vapor phase epitaxy *Appl. Phys. Express* **2** 5004
[18] Zhu J *et al* 2008 Optical absorption enhancement in amorphous silicon nanowire and nanocone arrays *Nano Lett.* **9** 279–82
[19] Anjia G *et al* 2010 Design and growth of III–V nanowire solar cell arrays on low cost substrates *PVSC: Photovoltaic Specialists Conf., 2010 35th IEEE*
[20] Tamboli A C *et al* 2010 GaP/Si wire array solar cells *PVSC: Photovoltaic Specialists Conf., 2010 35th IEEE*
[21] Adachi M M, Anantram M P and Karim K S 2010 Optical properties of crystalline–amorphous core–shell silicon nanowires *Nano Lett.* **10** 4093–8
[22] Gunawan O *et al* 2011 High performance wire-array silicon solar cells *Prog. Photovolt., Res. Appl.* **19** 307–12
[23] Garnett E and Yang P 2010 Light trapping in silicon nanowire solar cells *Nano Lett.* **10** 1082–7
[24] Bi H and LaPierre R R 2009 A GaAs nanowire/P3HT hybrid photovoltaic device *Nanotechnology* **20** 465205
[25] Jiun-Jie C *et al* 2010 GaAs nanowire/poly(3,4-ethylenedioxythiophene): poly(styrenesulfonate) hybrid solar cells *Nanotechnology* **21** 285203
[26] Hu L and Chen G 2007 Analysis of optical absorption in silicon nanowire arrays for photovoltaic applications *Nano Lett.* **7** 3249–52
[27] Lin C and Povinelli M L 2009 Optical absorption enhancement in silicon nanowire arrays with a large lattice constant for photovoltaic applications *Opt. Express* **17** 19371–81
[28] Li J *et al* 2009 Si nanopillar array optimization on Si thin films for solar energy harvesting *Appl. Phys. Lett.* **95** 033102
[29] Kupec J and Witzigmann B 2009 Dispersion, wave propagation and efficiency analysis of nanowire solar cells *Opt. Express* **17** 10399–410
[30] Anttu N and Xu H Q 2010 Coupling of light into nanowire arrays and subsequent absorption *J. Nanosci. Nanotechnol.* **10** 7183–7
[31] Gu Z *et al* 2011 On optical properties of GaAs and GaAs/AlGaAs core–shell periodic nanowire arrays *J. Appl. Phys.* **109** 064314
[32] Palik E D and Ghosh G 1998 *Handbook of Optical Constants of Solids* (New York: Academic)
[33] Filmetrics *Refractive Index Database* 2011 available from www.filmetrics.com/refractive-index-database/
[34] Adachi S, Capper P and Kasap S 2009 *Properties of Semiconductor Alloys: Group-IV, III–V and II–VI Semiconductors* (New York: Wiley)
[35] Adachi S 1999 *Optical Constants of Crystalline and Amorphous Semiconductors: Numerical Data and Graphical Information* (Netherlands: Springer)
[36] Li M *et al* 2006 Higher-order incidence transfer matrix method used in three-dimensional photonic crystal coupled-resonator array simulation *Opt. Lett.* **31** 3498–500

[37] Li M *et al* 2006 High-efficiency calculations for three-dimensional photonic crystal cavities *Opt. Lett.* **31** 262–4
[38] Pendry J B 1994 Photonic band structures *J. Mod. Opt.* **41** 209–29
[39] Whittaker D M and Culshaw I S 1999 Scattering-matrix treatment of patterned multilayer photonic structures *Phys. Rev.* B **60** 2610
[40] Shockley W and Queisser H J 1961 Detailed balance limit of efficiency of p–n junction solar cells *J. Appl. Phys.* **32** 510–9
[41] ASTM *Reference Solar Spectral Irradiance: Air Mass 1.5 Spectra* available from http://rredc.nrel.gov/solar/spectra/am1.5
[42] Li Y *et al* 2006 Dopant-free GaN/AlN/AlGaN radial nanowire heterostructures as high electron mobility transistors *Nano Lett.* **6** 1468–73
[43] Wong B M, Leonard F, Li Q and Wang T G 2011 Nanoscale effects on heterojunction electron gases in GaN/AlGaN core/shell nanowires *Nano Lett.* **11** 3074–9